Journal of
Nanoscience and Nanotechnology
Vol. 13, 6429–6433, 2013

Growth of Semipolar InGaN Quantum Well Structure Using Self-Organized Nano-Masks on *m*-Sapphire

Yongwoo Ryu, Joocheol Jeong, Jongjin Jang, Kyuseung Lee, Daehong Min, Jinwan Kim, Minho Kim, Seunghwan Moon, Geunho Yoo, and Okhyun Nam*

LED Technology Center, Department of Nano-Optical Engineering, Korea Polytechnic University, Siheung 429-793, Korea

This paper reports the improved microstructural and optical properties of semipolar (11–22) InGaN quantum well (QW) structures grown on SiO_2 nanorods formed by introducing self-organized masks. The crystal quality of GaN grown on SiO_2 nanorods was significantly improved by the defect blocking mechanism. The cathodoluminescence (CL) intensity of regrown GaN on SiO_2 nanorods increased approximately 9.5 times in comparison with that of the reference GaN, which is attributed to the defect reduction effect of the nanorods. Semipolar InGaN/GaN double QWs grown on SiO_2 nanorod masks showed an approximately 80% increase in internal quantum efficiency (IQE) in relation to that of the reference GaN.

Keywords: MOCVD, Semipolar, Nanorod, GaN.

RESEARCH ARTICLE

1. INTRODUCTION

InGaN-based optoelectronic devices such as light-emitting diodes and laser diodes are conventionally grown on *c*-plane sapphire substrates. However, these devices suffer from the quantum-confined stark effect (QCSE) because of the existence of spontaneous and piezoelectric polarization fields.[1, 2] Because the QCSE leads to a reduction in the internal quantum efficiency (IQE), which is attributed to a decrease in the overlap of electron and hole wave functions in the quantum wells, nonpolar and semipolar GaN growth have been widely investigated in order to avoid the polarization effect.[3, 5–8] However, the limitation of nonpolar and semipolar GaN growth is that no suitable substrate can be used for hetero-epitaxial GaN growth. For example, the defect density of semipolar (11–22) GaN directly grown on *m*-plane sapphire substrates is typically high, with values on the order of 10^{10} cm^{-2} for dislocations and 10^5 cm^{-1} for basal stacking fault (BSFs).[8–10]

Therefore, various defect reduction techniques such as patterned sapphire substrates (PSSs),[4] epitaxial lateral overgrowth (ELO),[11, 12, 16] and nanoporous GaN by photoenhanced electrochemical etching have been used to improve the crystal quality of semipolar GaN layers.[13] Above all, it has been known that the ELO method is an effective technique for producing high-quality films suitable for growing quantum structures, despite the difficulty in the coalescence of semipolar (11–22) GaN. In this study, we suggest that ELO on SiO_2 nanorods using self-organized masks can be utilized to reduce the defects in semipolar InGaN quantum well (QW) structure growth.[16]

2. EXPERIMENTAL DETAILS

A semipolar GaN template (11–22) GaN was grown on a (10–10) *m*-plane sapphire substrate using metal–organic chemical vapor deposition (MOCVD). Trimethylgallium (TMGa), trimethylindium (TMIn), and ammonia (NH_3) were used as precursors. After thermal cleaning of the sapphire substrate in H_2 and NH_3 at 1090 °C, a high-temperature buffer layer was grown on the substrate, followed by 2 μm growth of (11–22) GaN at 1040 °C. For the subsequent overgrowth, self-organized nanorods were fabricated on the abovementioned semipolar GaN template, as illustrated in Figure 1.

First, a 100-nm-thick SiO_2 layer was deposited on the semipolar GaN template by plasma-enhanced chemical vapor deposition (PECVD). A 15 nm thick Au film was evaporated, subsequently, on the SiO_2 layer using sputtering [Fig. 1(b)], followed by a rapid thermal annealing (RTA) with N_2 atmosphere at 850 °C for 2 min to form self-organized Au nanoclusters [Fig. 1(c)]. The Au nanoclusters functioned as a mask to etch the underlying SiO_2 film using inductively coupled plasma (ICP) in

*Author to whom correspondence should be addressed.

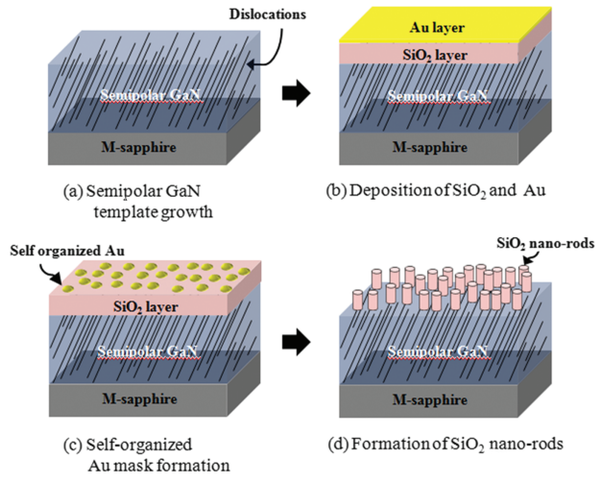

Fig. 1. The schematic of experimental procedure.

order to make SiO_2 nanorods on GaN. Two kinds of samples were prepared by controlling the etching time in this process in order to obtain different coverage amounts of SiO_2 nanorods (see Fig. 2). The Au nanoclusters were removed by aqua regia ($HCl:HNO_3 = 3:1$), leaving the SiO_2 nanorods on the semipolar GaN [Fig. 1(d)]. Then, the semipolar GaN template with the SiO_2 nanorod structures was again subjected to MOCVD for overgrowth. The growth conditions such as the pressure and flow rates of the metal–organic sources were optimized to obtain good morphology on the GaN template with the nanorod layer. The total thickness of the semipolar GaN layer was approximately 5 μm. Finally, InGaN/GaN double quantum wells (DQWs) were grown on both the reference and the SiO_2 nanorod-embedded GaN. The DQWs consisted of 3.5-nm-thick InGaN wells and 12-nm-thick GaN barriers. The surface and cross-section morphology of the semipolar GaN layers were observed by scanning electron microscopy (SEM). High-resolution double-crystal X-ray rocking curves (DCXRCs) were measured for the on- and off-axis planes of the semipolar GaN layers. A cathodoluminescence (CL) analysis was conducted to investigate the luminescence characteristics of the semipolar GaN. The InGaN DQW structures were analyzed by temperature-dependent photoluminescence (TD-PL).

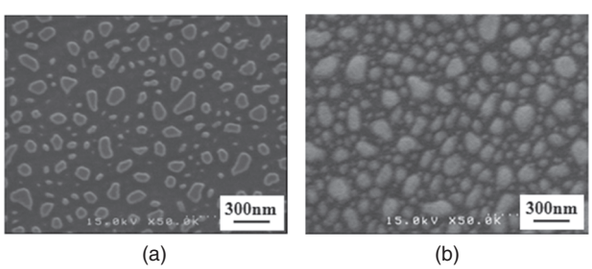

Fig. 2. The SEM images of SiO_2 nano-rods on semipolar GaN layers. The coverages of SiO_2 are (b) 25% and (c) 45%, respectively.

3. RESULTS AND DISCUSSION

Figures 2(a) and (b) show the plan-view SEM images of the SiO_2 nanorods with coverages of 25% and 45%, respectively, on the semipolar GaN layers. The diameter of the nanorods varied from 50 nm to 150 nm, which was similar in both samples.

Figure 3 shows the plan-view SEM images and monochromatic CL images of the reference and semipolar GaN layers grown on SiO_2 nanorods.

The surface morphology of all samples showed arrowhead-like features, which could be modified by the incorporation probability and the diffusion length of surface adatoms toward anisotropic crystallographic directions such as [11–2–3] and [−1100], because of the crystallographic difference between *m*-plane (1–100) sapphire and semipolar (11–22) GaN.[17–18] Moreover, the arrowhead-like features of the semipolar GaN on SiO_2 nanorods on GaN became larger than those of the reference GaN, which is caused by the increase in the surface migration length of Ga atoms due to the decrease in defect density.[19]

The CL images in Figures 3(d)–(f) show dark and bright patterns corresponding to high and low defect regions, respectively. These data indicate that the crystal quality was significantly improved in the semipolar GaN on SiO_2 nanorods with 45% coverage.

Figure 4 shows the full width at half maximums (FWHMs) of XRCs of the on- and off-axis planes of the reference and the SiO_2 nanorod-embedded GaN.

The FWHM broadening of the on-axis rocking curves of (11–22) with diffraction directions of [−1–123] and [1–100] was reported to be related to partial dislocations(PDs) and to PDs and/or prismatic stacking faults (PSFs), respectively.[20]

The FWHMs of the on-axis plane (11–22) with a diffraction direction of [−1–123] for the reference and the SiO_2 nanorod-embedded GaN samples with coverages of 25%, and 45% were 1200, 1100, and 850 arcsec, respectively. In addition, the FWHMs of the on-axis plane (11–22) with a diffraction direction of [1–100] for the reference and the SiO_2 nanorod-embedded GaN samples were similar to those for the [−1–123] direction. These results indicate that the SiO_2 nanorods reduced existent PDs and/or PSFs in the GaN layers. Then, the FWHMs of the off-axis planes such as (0002) and (10–10) were measured to investigate PDs/perfect dislocation and BSFs.[20] The FWHMs of the SiO_2 nanorod-embedded GaN with coverages of 25%, and 45% decreased by approximately 30% and 50% in the (0002) plane, respectively, and by 4% and 26% in the (10–10) plane, respectively, compared with the FWHMs of the reference. These results suggest that the SiO_2 nanorods block defects such as PDs and/or perfect dislocation and BSFs. The remarkable decrease in the FWHMs of the (0002) plane, in particular,

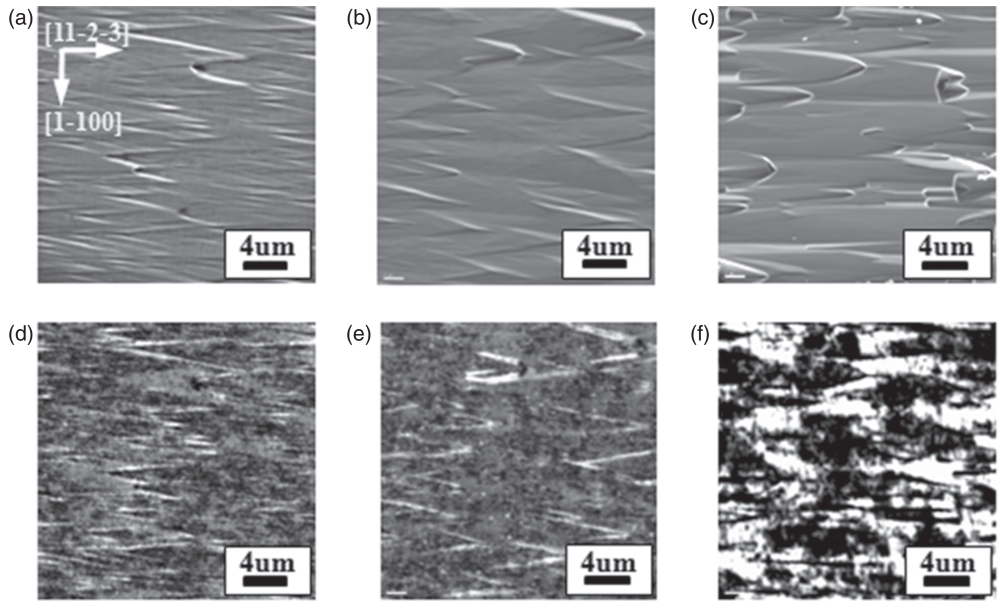

Fig. 3. The SEM [(a)–(c)] and CL [(d)–(f)] images of the reference [(a), (d)] and the semipolar GaN layers grown on SiO_2 nano-rods. The coverages of SiO_2 are [(b), (e)] 25% and [(c), (f)] 45%, respectively.

shows a considerable reduction in PDs and/or perfect dislocations.

Moreover, we could calculate the BSF density on the basis of the XRD results using a Williamson–Hall plot, which is used to separate the lateral coherence length (LCL) broadening and dislocation broadening on XRCs with Lorentzian distribution.[14–15]

According to the Williamson–Hall plot method,[15] LCLs for the reference and the SiO_2 nanorod-embedded GaN samples with coverages of 25% and 45% were 25 nm, 32 nm, and 54 nm, respectively, and the BSF densities were 3.9×10^5 cm^{-1}, 3.1×10^5 cm^{-1}, and 1.8×10^5 cm^{-1}, respectively. Our DCXRC measurements suggest that the density of defects such as dislocations and BSFs was greatly reduced by using SiO_2 nanorods in grown semipolar GaN.

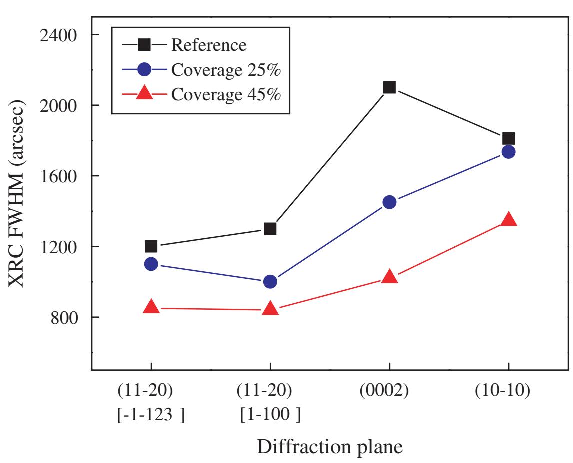

Fig. 4. The FWHMs of X-ray rocking curves of on- and off-axis planes of the semipolar GaN layers.

Figures 5(a) and (b) show SEM and CL images, respectively, of the cross-section of the SiO_2 nanorodembedded GaN sample with 45% coverage.

SiO_2 nanorods layers are clearly seen in Figure 5(a). The cross-section CL image shows that the upper layer of GaN overgrown on the nanorods is brighter than that of the lower GaN template layer. In addition, as shown in Figure 5(c), the CL intensity of spot 2 was 9.5 times higher than that of spot 1, which indicates that the SiO_2 nanorods blocked the defects effectively.

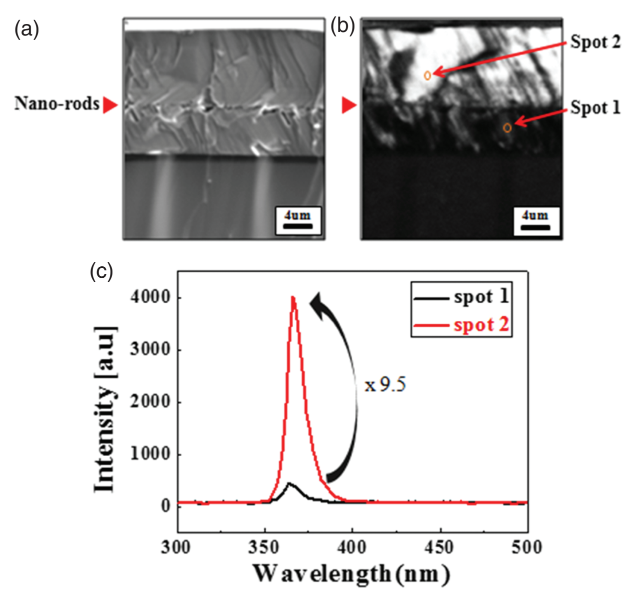

Fig. 5. The cross section (a) SEM and (b) CL image on the same area of the semipolar GaN grown on SiO_2 nano-rods with coverage of 45%. (c) shows the CL spectra on spot 1 and spot 2 in (b).

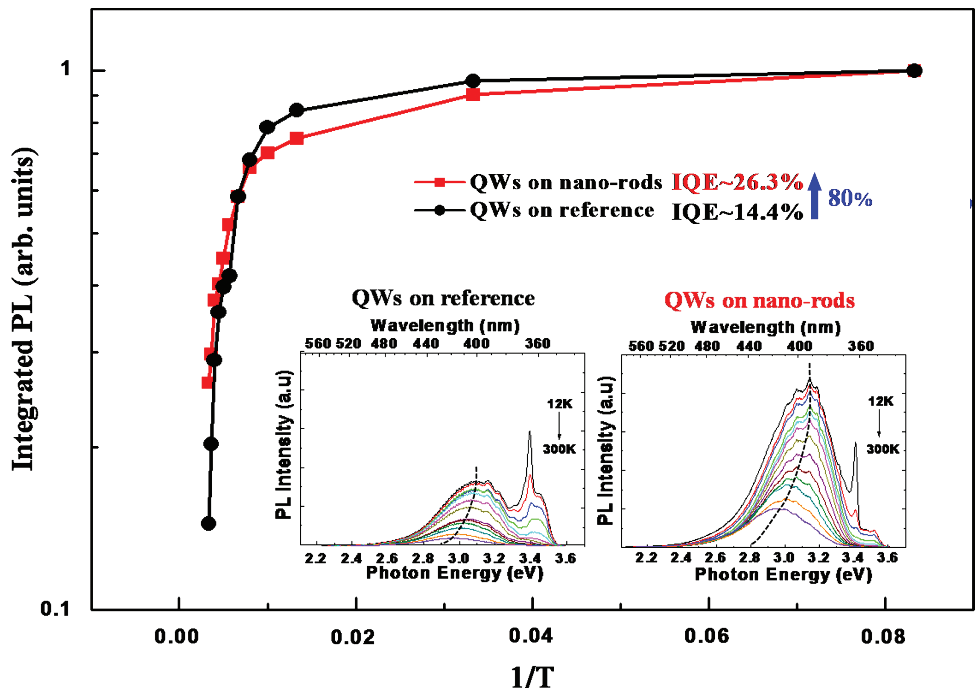

Fig. 6. Arrhenius plots of the normalized integrated PL data of reference and SiO_2 nano-rods embedded InGaN QWs. Insets show temperature dependent PL spectra of (a) reference and (b) SiO_2 nano-rods embedded InGaN QWs. (The coverage of SiO_2 is 45%.)

Figure 6 shows the normalized integrated PL data of InGaN DQWs grown on the reference sample and the SiO_2 nanorod-embedded GaN sample with 45% coverage as a function of temperature in Arrhenius plots for temperature ranging from 13 K to 300 K. The inset shows the temperature-dependent PL spectra of the two samples.

The calculated IQEs were approximately 14.4% and 26.3% for InGaN DQWs grown on the reference and the SiO_2 nanorod-embedded GaN samples, respectively. This means the IQE increased by approximately 80% in the case of the InGaN DQWs on SiO_2 nanorod-embedded GaN compared with that of the reference GaN.

4. CONCLUSION

In conclusion, we demonstrated an improvement in the crystal quality and optical properties of semipolar (11–22) GaN grown using SiO_2 nanorods. When semipolar GaN was grown on SiO_2 nanorods, the FWHMs of the XRCs of both the on- and off-axis planes significantly decreased and the monochromatic CL intensity increased owing to the reduction in defects. The cross-section CL image showed that the nanorod layers functioned as blocking masks of the defects, and the CL intensity of GaN overgrown on the nanorods increased approximately 9.5 times compared with that of the lower GaN. The IQE of the InGaN DQWs was enhanced from 14.4% to 26.3% by introducing the nanorod-embedded structure, which indicates an improvement in the crystal quality of semipolar GaN. The semipolar (11–22) GaN growth using SiO_2 nanorod technology is a promising method for fabricating high-performance semipolar GaN devices.

Acknowledgment: This work was supported by World Premier Materials Project No. 10037886 and the National Research Foundation of Korea (NRF) grant funded by the Korea government (MEST) No. 2012R1A2 A2A01011702.

References and Notes

1. T. Takeuchi, S. Sota, M. Katsuragawa, M. Komori, H. Takeuchi, H. Amano, and I. Akasaki, *Jpn. J. Appl. Phys.* 36, 382 **(1997)**.
2. D. A. B. Miller, D. C. Chemla, T. C. Damen, A. C. Grossard, W. Wiegmann, T. H. Wood, and C. A. Burrus, *Phys. Rev. B* 32, 1043 **(1985)**.
3. J. S. Im, H. Kollmer, J. Off, A. Sohmer, F. Scholz, and A. Hangleiter, *Phys. Rev. B* 57, 9435 **(1998)**.
4. J. Jang, K. Lee, J. Hwang, J. Jung, S. Lee, K. Lee, B. Kong, H. Cho, and O. Nam, *J. Cryst. Growth* 361, 166 **(2008)**.
5. S. Jung, S.-N. Lee, K. S. Ahn, and H. Kim, *Electronic. Mater. Lett.* 8, 1 **(2012)**.
6. Y. Lee, T. Seo, A. Park, K. Lee, S. Chung, and E. Suh, *Electron. Mater. Lett*, 8, 3 **(2012)**.
7. L. Lahourcade, E. Bellet-Amalric, E. Monroy, M. Abouzaid, and P. Ruterana, *Appl. Phys. Lett.* 90, 131909 **(2007)**.
8. T. J. Baker, B. A. Haskell, F. Wu, J. S. Speck, and S. Nakamura, *Jpn. J. Appl. Phys.* 45, L154 **(2006)**.
9. T. Gühne, Z. Bougrioua, P. Vennéguès M. Leroux, and M. Albrecht, *J. Appl. Phys.* 101, 113101 **(2007)**.
10. T. J. Baker, B. A. Haskell, F. Wu, J. S. Speck, and S. Nakamura, *Jpn. J. Appl. Phys.* 45, 154 **(2006)**.

11. Y. Kato, S. Kitamura, K. Hiramatsu, and N. Sawaki, *J. Cryst. Growth* 144, 133 **(1994)**.
12. M. Martyniuk, G. Parish, H. Marchand, P. T. Fini, S. P. DenBaars, and L. Faraone, *Electron. Mater. Lett*. 8, 2 **(2012)**.
13. D. H. Lee, J. J. Jang, B. H. Kong, H.-K. Cho, and O. Nam, *Jpn. J. Appl. Phys*. 49, 058001 **(2010)**.
14. J.-Q. Liu, Y.-X. Qiu, J.-F. Wang, K. Xu, and H. Yang, *Chin. Phys. Lett*. 28, 016101 **(2011)**.
15. M. B. Mclaurin, A. Hirai, E. Young, F. Wu, and J. S. Speck, *Jpn. J. Appl. Phys*. 47, 5429 **(2008)**.
16. K. Xing, Y. Gong, J. Bai, and T. Wang, *Appl. Phys. Lett*. 99, 181907 **(2011)**.
17. S.-N. Lee, K. K. Kim, O. H. Nam, J. H. Kim, and H. Kim, *Phys. Status Solidi C* 7, 2043 **(2010)**.
18. T. Wernicke, C. Netzel, M. Weyers, and M. Kneissl, *Phys. Status. Solidi. C* 5, 1815 **(2008)**.
19. S. Lee, J. Jang, K.-H. Lee, J.-H. Hwang, J. Jeong, and O. Nam, *Phys. Status Solidi A* 209, 1526 **(2012)**.
20. Q. Sun, B. Leung, C. R. D. Yerino, Y. Zhang, and J. Han, *Appl. Phys. Lett*. 95, 231904 **(2009)**.

Received: 5 October 2012. Accepted: 6 January 2013.